J Neuropathol Exp Neurol

Vol. 65, No. 12
December 2006
pp. 1170–1180

ORIGINAL ARTICLE

Fractalkine Expression in the Rhesus Monkey Brain During Lentivirus Infection and Its Control by 6-Chloro-2′,3′-Dideoxyguanosine

Candan Depboylu, MD, Lee E. Eiden, PhD, Martin K.-H. Schäfer, MD, Todd A. Reinhart, PhD, Hiroaki Mitsuya, PhD, Thomas J. Schall, PhD, and Eberhard Weihe, MD

Abstract

Existing data concerning the role of the δ-chemokine fractalkine (CX3CL1) and its receptor (CX3CR1) in lentivirus-induced encephalitis are limited and controversial. We explored, by quantitative in situ hybridization and immunohistochemistry, the cell-specific changes of CX3CL1 and CX3CR1 in rhesus macaque brain during simian immunodeficiency virus (SIV) infection and antiretroviral treatment. Neuronal expression of CX3CL1 was significantly reduced in cortex and striatum of AIDS-diseased monkeys as compared with uninfected and asymptomatic SIV-infected monkeys. CX3CL1 mRNA was increased in some endothelial cells and newly induced in astrocytes and macrophages focally in areas of SIV burden and inflammatory infiltrates. In most CX3CL1-positive astrocytes and macrophages, the transcription factor NF-κB was translocated to the nucleus. CX3CR1 was upregulated in scattered, nodule, and giant cell-forming microglia/macrophages and mononuclear infiltrates close to CX3CL1-induced cells in the brain. Treatment of AIDS monkeys with the central nervous system-permeant 6-chloro-2′,3′-dideoxyguanosine fully reversed SIV burden, productive inflammation, nuclear NF-κB translocation as well as focal induction of CX3CL1 in astrocytes and macrophages and downregulation in neurons. In contrast, diffuse CX3CR1-positive microgliosis and GFAP-positive astrogliosis were partially reversed by 6-chloro-2′,3′-dideoxyguanosine. Thus, focally induced CX3CL1 may be a target for therapeutic intervention to limit ongoing inflammatory infiltration into brain in lentivirus infection.

From the Department of Molecular Neuroscience (CD, MK-HS, EW), Institute of Anatomy and Cell Biology and the Department of Neurology (CD), Center for Nervous Diseases, Philipps University, Marburg, Germany; the Section on Molecular Neuroscience (LEE), Laboratory of Cellular and Molecular Regulation, National Institute of Mental Health, National Institutes of Health, Bethesda, MD; the Department of Infectious Diseases and Microbiology (TAR), University of Pittsburgh, Pittsburgh, PA; the Division of Cancer Treatment (HM), National Cancer Institute, National Institutes of Health, Bethesda, MD; and the Division of Discovery Biology and Molecular Pharmacology (TJS), ChemoCentryx, San Carlos, CA.

Send correspondence and reprint requests to: Dr. Eberhard Weihe, Institute of Anatomy and Cell Biology, Department of Molecular Neuroscience, Philipps University, Robert-Koch-Str. 8, 35032 Marburg, Germany; E-mail: weihe@staff.uni-marburg.de

This study was supported by the Volkswagen Foundation to L. E. Eiden and E. Weihe and by the Integrative Neural-Immune Program (INIP), NIMH-IRP to L. E. Eiden.

Key Words: Antiretroviral treatment, Chemokine, Gliosis, Infiltration, Neuro-AIDS, Neuroinflammation.

INTRODUCTION

Monkeys infected with simian immunodeficiency virus (SIV) develop acquired immunodeficiency syndrome (AIDS) and neurologic symptoms similar to those of human immunodeficiency virus (HIV)-infected individuals (1). SIV-induced encephalitis is characterized by general gliosis, nodule and giant cell formation, inflammatory cell infiltrates, myelin pallor, and vessel leakage (2–5). Loss of synapses, dendrites, and neurons also occurs in SIV disease (6–8). Neurodegenerative damage could be caused by virus-derived as well as host-derived neurotoxic products (7) and is thought to be related to SIV replication and the number of inflammatory cells infiltrating and becoming activated in the brain (8, 9).

The activation, recruitment, and trafficking of inflammatory cells are controlled by chemokines (10). Fractalkine is the only known δ-chemokine (11, 12) also designated as CX3CL1 (13). It exists either in a membrane-anchored or a soluble form and acts as a chemoattractant and as an adhesion molecule through its G-protein-coupled receptor CX3CR1 (14, 15). CX3CL1 and CX3CR1 are constitutively expressed in the brain (11, 12, 16–19). Fractalkine is elevated in the cerebrospinal fluid (CSF) of HIV-diseased individuals compared with individuals with other neurologic symptoms or with healthy controls (20). Individuals with HIV-associated dementia have higher levels of CX3CL1 in the CSF than HIV-infected patients without dementia (21). The sites of CX3CL1 expression during HIV brain inflammation responsible for the increased release of CX3CL1 into CSF are not yet identified (22, 23), limiting further understanding of the role of CX3CL1 in lentiviral encephalopathy.

We assessed the relationship between brain virus burden and associated neuroinflammatory reactions and altered cerebral expression of CX3CL1 and CX3CR1 in the SIV-macaque model of HIV infection and during treatment with the CNS-permeant antiretroviral agent 6-chloro-2′,3′-dideoxyguanosine (6-Cl-ddG) (24–26) to determine the sites of expression and potential role of the δ-chemokine in an experimentally tractable model for neuro-AIDS (1, 3). Our

data suggest distinct routes of SIV neuropathogenesis involving brain-derived CX3CL1 in separate cellular compartments that should be considered in potential treatment strategies in neuro-AIDS.

MATERIALS AND METHODS

Virus Stock, Inoculation Procedures, Antiretroviral Treatment, and Tissue Preparation for Histochemical Analysis

Procedures performed on the juvenile rhesus macaque monkeys have been described previously (25, 26). Experiments involving the use of rhesus macaques were approved by the Animal Care and Use Committee of Bioqual, Inc., a National Institutes of Health (NIH)-approved and Association for Assessment and Accreditation of Laboratory Animal Care-accredited research facility. All experiments were carried out using the ethical guidelines promulgated in the NIH Guide for the Care and Use of Laboratory Animals. Healthy juvenile rhesus macaques were inoculated intravenously with 10 rhesus infectious doses of cell-free $SIV_{\delta B670}$ (27). At the time of euthanasia, 8 macaques exhibited clinical signs of AIDS and 5 did not (25, 26). Four age-matched noninfected macaques were used as controls. Additionally, a group of 4 monkeys that were antiretrovirally treated with 6-Cl-ddG and had clinical signs of AIDS were analyzed (25, 26). Study details are summarized in Table 1. At the time of death, anesthetized animals were perfused transcardially with phosphate-buffered saline (PBS) and formalin/PBS. Tissue specimens were obtained during necropsy and immersion-fixed overnight. Some blocks were cryopreserved in sucrose and snap-frozen in ice-cooled isopentane. Some blocks were postfixed in Bouin-Hollande solution and processed for paraffin embedding (25, 26).

Single and Double Immunohistochemistry

Immunohistochemistry (IHC) was carried out on deparaffinized paraffin-embedded tissue sections (7 μm) or cryosections (14 μm) using an antigen retrieval technique

TABLE 1. List of Monkeys With Treatment Regime, Brain Virus Burden, Focal and Global Mononuclear, and Astroglial Reactions in the Brain as Well as Clinical Findings at the Time of Death and Necropsy*

Monkey Number	Antiretroviral Treatment	Brain SIV Burden§	Mononuclear Reactions‖		Astroglial Reactions¶		Clinical Findings
			Focal	Global	Focal	Global	
44	Not treated	−	−	−	−	−	No disease
50	Not treated	−	−	−	−	−	No disease
69	Not treated	−	−	−	−	−	No disease
87	Not treated	−	−	−	−	−	No disease
75	Not treated	−	−	−/+	−	−	Asymptomatic
80	Not treated	−	−	+	−	−	Asymptomatic
85	Not treated	−	−	+	−	−	Asymptomatic
92	Not treated	−	−	+	−	−/+	Asymptomatic
93	Not treated	−	−	+	−	−	Asymptomatic
46	Not treated	+	+	+	+	+	Diarrhea, mycotic infection, mass
71	Not treated	++	++	++	++	++	Diarrhea, listless, rash
74	Not treated	+++	+++	++	+++	++	Diarrhea, anemia, parasitic infection, LN atrophy
78	Not treated	+++	+++	+++	+++	+++	Diarrhea, parasitic infection, pneumonitis
79	Not treated	+	+/++	++	+	+/++	Rash, heart murmur, LN atrophy
82	Not treated	+++	+++	+++	+++	+++	Diarrhea, wasting
86	Not treated	+++	+++	+++	+++	+++	Wasting, mass, thrush, colitis, LN atrophy
90	Not treated	++	++	++	+/++	++	Vomiting, wasting, tube feed
76†	ddI/6-Cl-ddG	−	−	++	−	++	Wasting, diarrhea, heart murmur, anemia
77†	ddI/6-Cl-ddG	−/+	−/+	++	−/+	++	Incontinence, wasting, diarrhea
89‡	6-Cl-ddG	−	−	+	−	+	Anemia, wasting, diarrhea, lymphoma
91†	ddI/6-Cl-ddG	−	−	+	−	+	Wasting, diarrhea

*, See also Depboylu et al (25, 26).

†, Treatment with ddI prior to the central nervous system-permeant 6-Cl-ddG.

‡, Treatment only with 6-Cl-ddG.

§, Detection of SIV *env*/*pol* by ISH and detection of SIV *gp41* and *gag* by IHC; scoring was as follows: − (no positive cells) to +++ (increasing number and/or signal/staining intensity of cells).

‖, Mononuclear reactions monitored by IHC for Iba1 and CX3CL1, and ISH for CX3CR1 and CX3CL1 in this study, and for C1q, indoleamine-2,3-dioxygenase, CD-68 in our previous studies (25, 26); for focal mononuclear reactions, scoring was: − (no appearance of infiltrates, nodules, and multinucleated giant cells), + (low) to +++ (severe encephalitis, high number of infiltrates, nodules, and multinucleated giant cells); for global mononuclear reactions, scoring was: − (no signs of activation, more resting ramified type of microglia), + (activated ameboid type cells with shortened ramifications), ++ (moderate) to +++ (strong activation, phagocytic type of cells).

¶, Astroglial reactions monitored by IHC and ISH for GFAP and CX3CL1; for focal astroglial reactions scoring was: − (no reactive perivascular astrocytes), + (low) to +++ (high incidence of focal reactive astrocytes); for global astroglial reactions, scoring was: − (no signs of activation, rare fine resting type of astrocytes); + (mild) to +++ (strong activation, increasing number of hypertrophied astrocytes). The number of cells were not specifically determined. Sections from several brain regions were analyzed and summarized.

ddG, 6-chloro-2′,3′-dideoxyguanosine; ddI, 2′,3′-diodeoxyinosine; LN, lymph node; SIV, simian immunodeficiency virus.

TABLE 2. Quantitative Analysis of Neuronal CX3CL1 Protein and mRNA Expression in the Brain During Simian Immunodeficiency Virus Infection and Antiretroviral Treatment

	Ctrl	SIV,-AIDS	SIV,+AIDS	SIV,+AIDS,+ddG
Relative optical density (ROD)				
Frontal cortex	0.717 ± 0.03	0.667 ± 0.02	0.353 ± 0.03†	0.583 ± 0.01*
Insular cortex	0.620 ± 0.01	0.580 ± 0.03	0.447 ± 0.02†	0.533 ± 0.02
Occipital cortex	0.593 ± 0.02	0.610 ± 0.02	0.427 ± 0.04†	0.530 ± 0.03*
Entorhinal cortex	0.513 ± 0.01	0.527 ± 0.03	0.460 ± 0.02†	0.507 ± 0.02
Hippocampus	0.533 ± 0.02	0.520 ± 0.01	0.490 ± 0.02	0.503 ± 0.03
Thalamus	0.503 ± 0.01	0.513 ± 0.01	0.453 ± 0.03*	0.497 ± 0.02
Striatum	0.470 ± 0.02	0.463 ± 0.02	0.377 ± 0.02†	0.450 ± 0.01
Grain number				
Frontal cortex	199.0 ± 7.8	191.7 ± 4.7	128.0 ± 4.0†	183.0 ± 3.6*
Insular cortex	163.3 ± 4.5	158.3 ± 4.0	132.3 ± 3.1†	156.3 ± 5.1
Occipital cortex	172.0 ± 4.0	167.3 ± 3.2	140.3 ± 2.1†	162.0 ± 4.4
Entorhinal cortex	157.3 ± 4.0	161.0 ± 1.0	142.7 ± 2.1†	153.0 ± 1.0
Hippocampus	156.7 ± 4.2	160.3 ± 5.5	150.7 ± 5.1	151.3 ± 4.0
Thalamus	150.7 ± 4.0	152.3 ± 3.1	139.3 ± 2.5*	143.7 ± 1.5*
Striatum	156.3 ± 4.2	161.7 ± 2.1	133.3 ± 3.8†	147.0 ± 5.3

Analysis of variance and the post hoc Newman-Keuls multiple comparison test are used to evaluate statistical differences. The mean values and the variation (± standard deviation) are given.

*, Statistically significantly different only as compared with Ctrl and SIV,-AIDS groups for the same brain area ($p < 0.05$).

†, Statistically significantly different as compared with the other animal groups for the same brain area ($p < 0.05$).

Ctrl, control; SIV, simian immunodeficiency virus; AIDS, acquired immune deficiency syndrome.

and visualized enzymatically with 3,3′-diaminobenzidine (DAB; Sigma, Deisenhofen, Germany), enhanced by addition of ammonium nickel sulfate (Fluka, Buchs, Switzerland), or visualized by immunofluorescence, as previously described (25, 26). The following antibodies were used: a rabbit polyclonal antibody against the N-terminus of fractalkine (11, 19), a polyclonal antibody from guinea pig against glial fibrillary acid protein (GFAP; Progen, Heidelberg, Germany), a mouse monoclonal antibody recognizing CD3 (DAKO, Hamburg, Germany), a rabbit polyclonal antibody against von Willebrand factor (vWF; DAKO), a mouse monoclonal antibody against neuronal nuclear antigen (NeuN; Chemicon International, Temecula, CA), a rabbit polyclonal antibody recognizing the ionized calcium-adapter binding molecule (Iba1; a gift from Y. Imai, Department of Neurochemistry, National Institute of Neuroscience, Tokyo, Japan) (28), and a goat polyclonal antibody against NF-κB (Santa Cruz Biotechnology, Santa Cruz, CA). Double enzymatic IHC or double immunofluorescence was carried out as described previously (25, 26). Serial immunostaining was carried out on adjacent sections. Fluorescence signals were analyzed and documented with the Olympus AX70 microscope or with the Olympus Fluoview confocal laser scanning microscope (Olympus Optical, Hamburg, Germany).

Generation of Riboprobes, Radioactive and Nonradioactive In Situ Hybridization, Combination of Immunohistochemistry With In Situ Hybridization

Because rhesus monkey and human chemokine genes are highly homologous (29), human-specific riboprobes were generated to perform in situ hybridization (ISH) on rhesus monkey tissue sections. CX3CL1 (accession no. NM002996) and CX3CR1 (accession no. NM001337) were amplified by polymerase chain reaction directly from isolated human genomic DNA as template (Blood DNA Isolation Kit; Qiagen, Hilden, Germany) with AmpliTaq DNA polymerase (Applied Biosystems, Foster City, CA). The following primers were used: 5′-GGGCACCAGGACATATGAAT-3′ and 5′-TTGGAGACGAGACAGCACA-3′ for CX3CL1, 5′-TGGATCAGTTCCCTGAATCA-3′ and 5′-AAGGAG-CAATGCATCTCCAT-3 for CX3CR1. Amplified DNA fragments (approximately 1 kb for CX3CL1 and 1.1 kb for CX3CR1) were subcloned in the pGEM-T Easy Vector (Promega, Madison, WI).

A pBluescript SK-vector containing a 2.3-kb cDNA fragment of human GFAP (accession no. NM002055; obtained from ATCC, LGC Promochem, Wesel, Germany) and a pBluescript KS+ vector containing a 0.7 kb cDNA fragment of C1q alpha polypeptide (C1q A; accession no. NM015991; provided by W. J. Schwaeble, Department of Infection, Immunity and Inflammation, Leicester, U.K.) (26) were also used. For ISH, cryosections (14 μm) were cut from cryopreserved brain tissues and processed as previously reported (25). Specific sense and antisense riboprobes were generated from the linearized vector constructs by in vitro transcription using the appropriate RNA polymerases and [^{35}S]-UTP and digoxigenin-UTP as label and applied on sections after limited alkaline hydrolysis. After application of [^{35}S]-riboprobes, radioactive signals were detected by autoradiography on Hyperfilm β-max (Amersham Bioscience, Freiburg, Germany) for 1 to 4 days to estimate further exposure time when coating sections with NTB-2 nuclear emulsion (Eastman Kodak, Rochester, NY). For visualization of nonradioactive hybrids, the digoxigenin

detection method (Roche Diagnostics, Mannheim, Germany) was performed. Detection of 2 different RNA transcripts in the same tissue section was performed with radioactive and nonradioactive labeled riboprobes (26, 30). For visualizing of one or 2 antigens with an RNA transcript in the same tissue section, single or double immunofluorescence was performed in combination with ISH (25, 26).

Detection of Viral mRNA and Protein

Viral transcription and translation were detected by ISH and IHC. The monoclonal antibodies KK41 and KK64 (NIH AIDS Research and Reference Program, Bethesda, MD) from mouse, which were raised against *gp41* and *gag* of SIV_{mac251}, respectively, were used to detect the cross-reacting *gp41* and *gag* from $SIV_{\delta B670}$, respectively (31). ISH was performed as reported (25, 32).

Quantification of In Situ Hybridization and Immunohistochemistry, Statistics

For quantification of ISH signals, the numbers of silver grains of CX3CL1 mRNA-positive neurons were counted on autoradiograms counterstained with cresyl violet. For quantification of the immunostaining intensity of CX3CL1-positive neurons, the relative optical density (ROD) was determined on CX3CL1-stained sections. Sections were analyzed under bright-field conditions at highest magnification using a digital camera (Spot RT Slider; Diagnostic Instruments, Inc., Sterling Heights, MI) and computer-assisted image analysis (MCID M4 image analysis system; Imaging Research Inc., St. Catherine's, Ontario, Canada). For ISH as well as IHC analyses, 3 interval sections per anatomic area were analyzed for each monkey, respectively. At least 50 random neurons with a visible nucleus were examined per area on a section. The number of grains was determined above the outlined cross-sectional area of each perikaryon with a visible nucleus using a threshold algorithm. Grain number was corrected by determination of background grain density on adjacent sections hybridized with the sense probe. The immunostained area of each perikaryon was outlined for ROD integration. Data were expressed as mean number (± standard deviation [SD]) of grains per neuron and as mean ROD (± SD) per neuron. Analysis of variance and the post hoc Newman-Keuls multiple comparison test were used to evaluate statistical differences between the groups. Values of $p < 0.05$ were considered statistically significant. Data for the analyzed brain areas are summarized in Table 2.

RESULTS

Expression of CX3CL1 in Neurons During Simian Immunodeficiency Virus Disease and Influence of Antiretroviral Treatment

CX3CL1 mRNA and protein were found to be constitutively expressed in virtually all of the cortical and subcortical gray matter regions of noninfected rhesus monkey brain (Ctrl). Throughout the cortex, CX3CL1 revealed a laminar patterning that is typical for neurons.

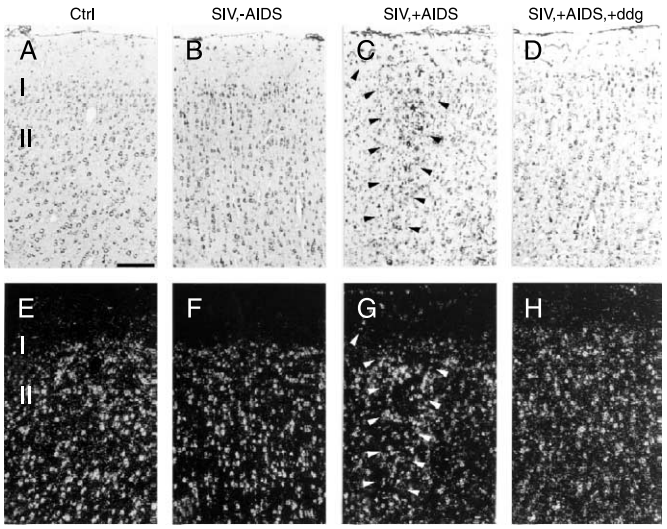

FIGURE 1. Changes of CX3CL1 protein and mRNA expression in the entorhinal cortex after simian immunodeficiency virus (SIV) infection and antiretroviral treatment demonstrated by representative **(A–D)** bright-field and **(E–H)** dark-field images of IHC and ISH for CX3CL1, respectively, performed on subjacent sections. **(A)** CX3CL1 protein and **(E)** mRNA are essentially restricted to neurons in a control monkey (Ctrl). Note focal induction in nonneuronal cells (arrowheads) and global reduction in neurons of **(C)** CX3CL1 protein and **(G)** mRNA in the SIV,+AIDS group as compared with **(A, E)** Ctrl and **(B, F)** SIV,-AIDS. These changes are abolished by antiretroviral treatment (SIV,+AIDS,+ddg; **[D, H]**). Scale bars = **(A–H)** 200 μm.

The analysis at cellular resolution confirmed the constitutive neuronal synthesis of CX3CL1 as demonstrated for the entorhinal cortex (Fig. 1A, E). SIV infection did not cause alterations of CX3CL1 expression in the brain in the early unproductive stage of disease relative to control (SIV,-AIDS; Fig. 1B, F). However, late stage of disease affected CX3CL1 transcript and protein expression in 2 different ways: 1) there was a decrease for CX3CL1 in neurons in most regions, especially in the cortex, and 2) there was focal induction in the white as well as in the gray matter as demonstrated for the entorhinal cortex (SIV,+AIDS; Fig. 1C, G). The focal de novo expression of CX3CL1 was observed in cells of nonneuronal morphology. Specificity of the antisense CX3CL1 riboprobe was assessed by ISH with the riboprobe in sense orientation, which showed only background signals. The absence of staining in preabsorption controls with excess recombinant CX3CL1 protein demonstrated the specificity of the antibody used.

To determine the influence of active viral burden, neuronal CX3CL1 expression was analyzed in brain tissue of AIDS-diseased rhesus monkeys that were treated with the antiretroviral agent 6-Cl-ddG. The decrease of neuronal CX3CL1 synthesis was reversed by 6-Cl-ddG (SIV,+AIDS,+ddG; Fig. 1D, H). No focal CX3CL1 mRNA expression was observed in the brain of antiretrovirally treated AIDS-symptomatic monkeys except some reactions in one monkey (Fig. 1D). CX3CL1 protein exhibited a

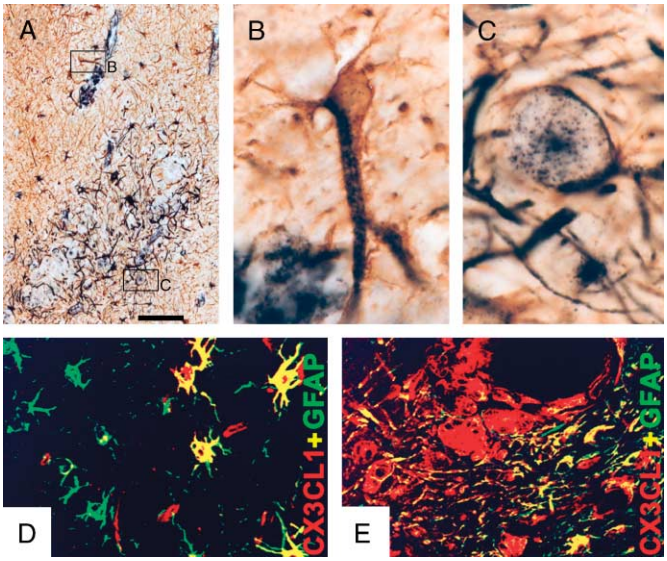

FIGURE 2. Identification of astrocytes and macrophages as sites of induction of CX3CL1 expression in SIV,+AIDS. **(A)** Representative low-power image demonstrating macrophage nodules, multinucleated giant cells, and mononuclear infiltrates in subcortical white matter. **(B, C)** High-resolution images from **(A)** showing polarized subcellular CX3CL1 immunoreactivity (dark blue) in hypertrophied GFAP-positive astroglial endfeet (brown) that is in close contact to CX3CL1-positive infiltrating macrophages **(B)** or to a CX3CL1-positive multinucleated giant cell **(C)**. **(D)** Confocal double immunofluorescence demonstrating CX3CL1 in perifocal astrocytes (red and green merged as yellow) besides CX3CL1-negative/GFAP-positive astrocytes (green). Note GFAP-negative/CX3CL1-positive vascular structures (red). **(E)** Confocal double immunofluorescence showing CX3CL1 in GFAP-negative macrophages and multinucleated giant cells (red) in the center of an inflammatory focus and in GFAP-positive astrocytes (red and green merged as yellow) in the immediate vicinity of the center of the inflammatory focus. Panels **(D)** and **(E)** are merged images. Scale bars = **(A)** 100 μm; **(B, C)** 10 μm; **(D, E)** 20 μm.

similar regulation pattern as its mRNA during SIV infection and antiretroviral treatment (Fig. 1H).

To quantify the differences of CX3CL1 expression in neurons between the experimental groups, ROD of CX3CL1 immunostaining and grain counts representing CX3CL1 mRNA were determined in neurons. In all regions examined, except the hippocampal formation and thalamus, both CX3CL1 protein and mRNA levels were significantly lower in the SIV,+AIDS group as compared with the other groups (Table 2).

Induction of CX3CL1 in Astrocytes and Cells of Mononuclear Origin During Simian Immunodeficiency Virus Disease and Influence of Antiretroviral Treatment

Analysis of IHC and ISH for CX3CL1 on sections throughout the brain of control as well as of infected monkeys without AIDS revealed a few occasional CX3CL1-positive microglial cells and astrocytes. In contrast, in SIV,+AIDS, there was an increase of CX3CL1 mRNA and protein in focally accumulating nonneuronal cells. To identify the cell types in which CX3CL1 is induced in terminal disease, costaining experiments were performed for CX3CL1 transcript and protein with established markers for brains resident cells. Enzymatic double IHC, double immunofluorescence, double ISH as well as a combination of immunofluorescence with ISH demonstrated clearly that CX3CL1 was focally de novo synthesized in astrocytes and in infiltrating macrophages and multinucleated giant cells in the brains of AIDS-symptomatic animals (Figs. 2 and 3). CX3CL1-positive astrocytes and macrophages exhibited close spatial relationships to blood vessels and to each other (Fig. 2). CX3CL1 immunoreactivity exhibited preferential accumulation in the hypertrophied astroglial endfeet processes (Fig. 2B). In addition, dual-labeling studies identified

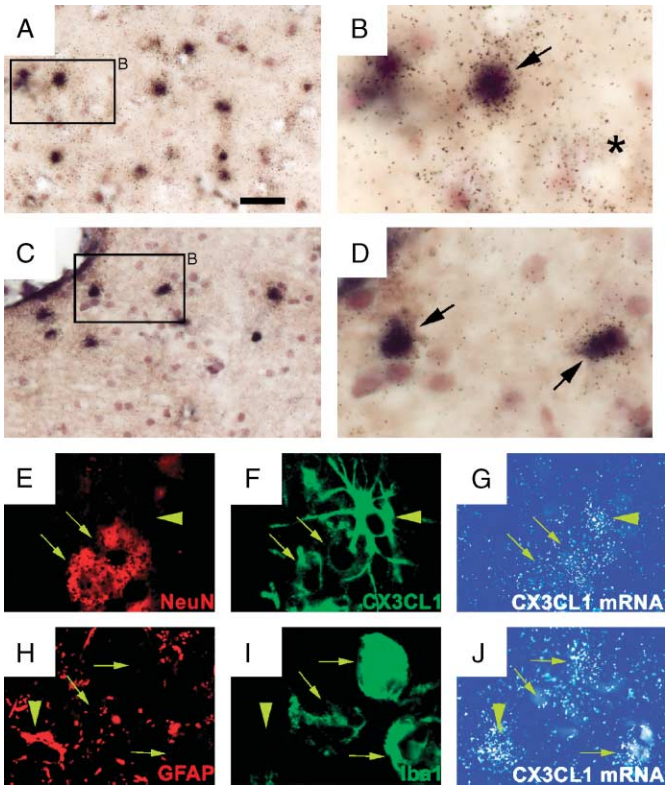

FIGURE 3. Colocalization of CX3CL1 mRNA and protein in neurons, astrocytes, and macrophages in SIV,+AIDS. Representative low- and high-power images demonstrating CX3CL1 mRNA (silver grains) in GFAP mRNA-positive (dark blue) astrocytes in cerebral cortex **(A, B)** and in subcortical white matter **(C, D)**. **(B, D)** Note CX3CL1 mRNA in GFAP-positive astrocytes (arrows) and at low levels in a GFAP-negative neuron (asterisk). Panels **(B)** and **(D)** are high-power images from **(A)** and **(C)**, respectively. **(E–J)** Combination of double immunofluorescence for NeuN, CX3CL1, GFAP, or Iba1 with ISH for CX3CL1 mRNA. Note CX3CL1 mRNA (grains) in NeuN/CX3CL1-copositive neurons (arrows in **[E–G]**) and in a CX3CL1-positive/NeuN-negative astrocyte (arrowhead in **[E–G]**), CX3CL1 mRNA in a GFAP-positive/Iba1-negative astrocyte (arrowhead in **[H–J]**) and in Iba1-positive/GFAP-negative macrophages (arrows in **[H–J]**). Scale bars = **(A, C)** 34 μm; **(B, D–J)** 10 μm.

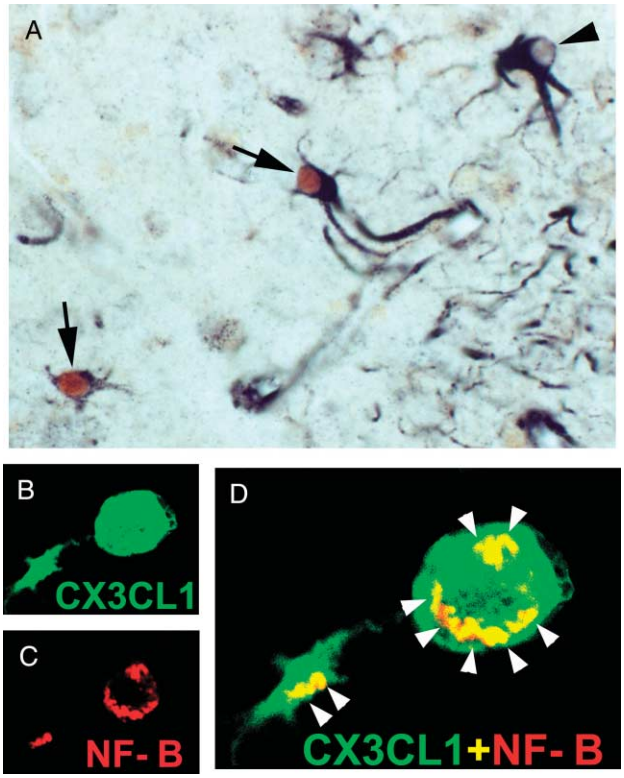

FIGURE 4. Nuclear translocation of NF-κB in CX3CL1-expressing astrocytes and macrophages in SIV,+AIDS. **(A)** Double enzymatic immunohistochemistry demonstrates nuclear NF-κB staining (brown, arrows) in 2 CX3CL1-positive astrocytes (dark blue) and absence in the nucleus (arrowhead) of another CX3CL1-positive astrocyte. **(B–D)** Confocal double immunofluorescence showing NF-κB (red) in the nucleus (arrowheads) of a CX3CL1-positive (green) astrocyte (lower left) and in a CX3CL1-positive multinucleated giant cell (upper right). Panels **(B)** and **(C)** are merged in **(D)**.

that in 90% to 95% of CX3CL1-positive astrocytes and cells of mononuclear origin, the transcription factor NF-κB was translocated to the nucleus (Fig. 4), suggesting possible NF-κB-dependent transcriptional induction of CX3CL1 in these cells. In multinucleated giant cells, CX3CL1 was coexistent with SIV (Fig. 5). The antiviral treatment fully reversed focal induction of CX3CL1 in astrocytes and macrophages, the increased nuclear translocation of NF-κB, SIV burden and the signs of productive inflammation in the brain of rhesus monkeys with AIDS. The effects of antiretroviral

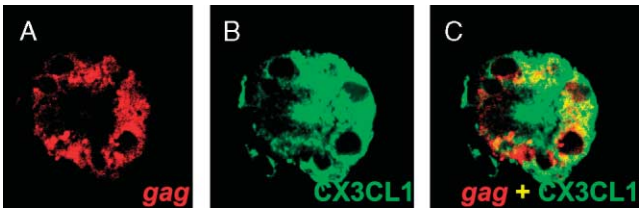

FIGURE 5. Confocal double immunofluorescence demonstrating colocalization of CX3CL1 (green) and simian immunodeficiency virus *gag* (red) in a multinucleated giant cell. Panels **(A)** and **(B)** are merged in **(C)**.

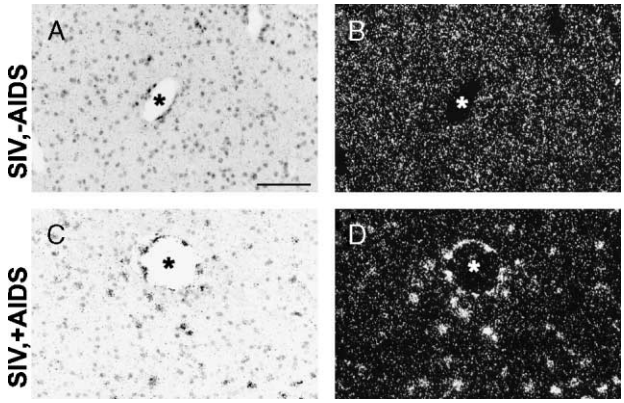

FIGURE 6. Representative **(A, C)** bright-field and **(B, D)** dark-field images of radioactive in situ hybridization for CX3CL1 in subcortical white matter during simian immunodeficiency virus (SIV) infection. Note induction of CX3CL1 mRNA in endothelial cells of a small blood vessel (asterisk) as well as in peri- and perivascular cells in SIV,+AIDS **(A, B)** as compared with SIV,-AIDS **(C, D)**. Scale bars = **(A–D)** 100 μm.

treatment on viral burden and mononuclear reactions, including the appearance of monocytic infiltrates, macrophage nodules, and multinucleated giant cells in the brain are summarized for all animals of the experimental groups in Table 1.

Expression of CX3CL1 in Endothelial Cells During Simian Immunodeficiency Virus Disease

CX3CL1 was found to be expressed in endothelial cells in noninfected rhesus monkey brain as revealed by serial immunostaining against von Willebrand factor (data not shown). During the course of lentiviral disease, the immunoreactivity of CX3CL1 in endothelial cells was not obviously changed in comparison to control. Antiretroviral treatment did not affect endothelial CX3CL1 staining intensity. ISH analysis revealed no detectable CX3CL1 mRNA in endothelial cells of uninfected monkeys and infected monkeys without AIDS (Fig. 6A, B). However, in the late stage of disease, CX3CL1 mRNA was increased in some endothelial cells of the brain (Fig. 6C, D). In antivirally treated monkey brain, CX3CL1 mRNA could not be detected in endothelial cells. Presence of CX3CL1 mRNA and protein in AIDS-symptomatic monkey brains indicates somewhat enhanced CX3CL1 synthesis, whereas absence of detectable levels of CX3CL1 mRNA is indicative of extremely low RNA synthesis of CX3CL1 in endothelial cells in nonsymptomatic and control animals.

Expression of CX3CR1 in Cells of Mononuclear Origin During Simian Immunodeficiency Virus Disease

To identify the cells that are receptive to CX3CL1, the cellular sites of CX3CR1 expression were determined by ISH on monkey brain tissue sections. CX3CR1 was constitutively expressed by microglia in brains of control and infected monkeys without AIDS (Fig. 7A, B). In SIV,+AIDS animals, the density and signal intensity of

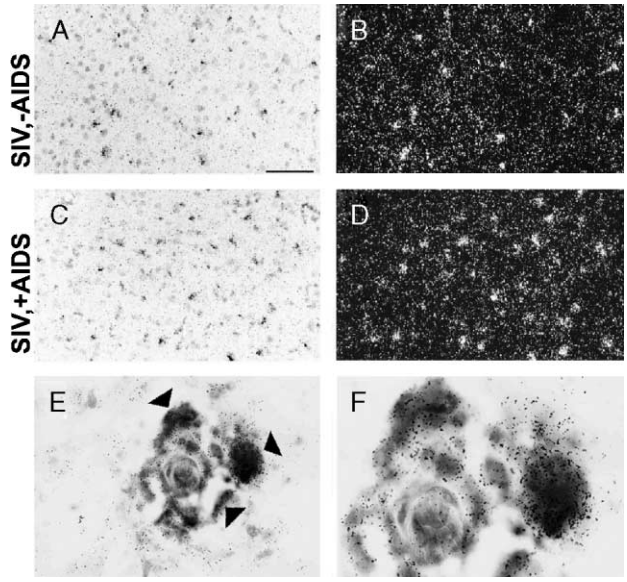

FIGURE 7. Cellular distribution and regulation of CX3CR1 in the brain during simian immunodeficiency virus infection. **(A, C)** Bright-field and **(B, D)** dark-field images of in situ hybridization for CX3CR1 mRNA representative for SIV,-AIDS and SIV,+AIDS. Note increase of CX3CR1 mRNA hybridization signals in scattered microglia/macrophage cells in **(C, D)** SIV,+AIDS as compared with **(A, B)** SIV,-AIDS. **(E, F)** Low- and high-resolution images of double-labeling ISH with [^{35}S]-labeled probes for CX3CR1 mRNA (silver grains) and digoxigenin-labeled riboprobes for C1q A mRNA (dark reaction product) demonstrating coexpression of CX3CR1 and C1q A in macrophages and multinucleated giant cells (arrowheads). Scale bars = **(A–D)** 80 μm; **(E)** 30 μm; **(F)** 15 μm.

CX3CR1 mRNA-positive cells were increased as compared with animals of Ctrl and SIV,-AIDS groups (Fig. 7C, D). CX3CR1 mRNA was synthesized mainly by diffuse distributed, nodule- and giant cell-forming as well as infiltrating cells of mononuclear origin identified by dual-labeling ISH for C1q A mRNA, as previously shown (26) (Fig. 7E, F). Antiretroviral treatment greatly diminished the appearance of CX3CR1-positive macrophage nodules, multinucleated giant cells, and infiltrates, but the density of diffuse CX3CR1-expressing microglia/macrophages was not fully reversed (Table 1). In contrast to the demonstrated preferential accumulation of macrophages in areas of CX3CL1-positive astrocytes, serial immunostaining and double immunostaining analyses for CX3CL1 and CD3, a marker for T-lymphocytes, revealed that there was no obvious or preferential accumulation of CD3-positive cells in areas of CX3CL1 induction in SIV encephalitis (data not shown).

Absence of CX3CL1 Expression in General Astrogliosis During Simian Immunodeficiency Virus Disease and Antiretroviral Treatment

Last, we investigated how the astrocytes lying outside of the CX3CL1-positive foci react in the monkey brain during the course of SIV infection and antiretroviral treatment. Therefore, sections of frontal cortex, occipital cortex, and entorhinal cortex of rhesus monkeys of all experimental groups were serially stained for CX3CL1 and the astroglial marker GFAP. In SIV,-AIDS monkey brains, no signs of general astroglial activation were observed as compared to controls (Fig. 8A, B). The brains of AIDS-diseased monkeys exhibited marked general astrogliosis as demonstrated by GFAP staining. However, in contrast to the presence of CX3CL1 in focally reactive astrocytes, CX3CL1 was completely absent from globally reactive astrocytes in the SIV,+AIDS group (Fig. 8C). Antiretroviral treatment resulted in some reduction but not abolishment of general GFAP-positive/CX3CL1-negative astrogliosis (Fig. 8D). The astrogliosis that persisted under antiretroviral treatment was also CX3CL1-negative. Table 1 summarizes focal and global astroglial and mononuclear reactions in the course of SIV disease and the effect of antiretroviral treatment.

DISCUSSION

The essential new findings of this study are as follows: 1) neuronal fractalkine (CX3CL1) expression is globally downregulated during SIV-induced encephalitis, especially in the cortex and striatum, and this downregulation is reversed by 6-Cl-ddG; 2) CX3CL1 is induced in macrophages and astrocytes in areas of SIV burden in late-stage

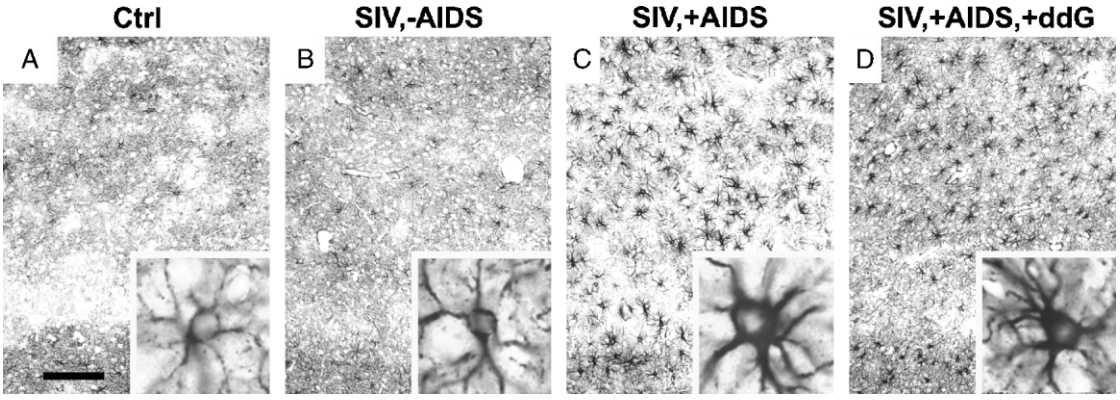

FIGURE 8. Astroglial reactions in the primary occipital cortex during simian immunodeficiency virus infection and antiretroviral treatment. Representative images of immunohistochemistry for GFAP demonstrate global astroglial activation in the **(C)** SIV,+AIDS group as compared with **(A)** Ctrl and **(B)** SIV,-AIDS. Astroglial activation persists in SIV,+AIDS,+ddG **(D)**. Scale bar = **(A–D)** 100 μm; insets = 17 μm.

AIDS and induction of CX3CL1 is abolished by 6-Cl-ddG; 3) fractalkine receptor (CX3CR1) expression is markedly enhanced in scattered and infiltrating cells of microglial/macrophage lineage that form nodules and syncytia in SIV-induced encephalitis; and 4) increased CX3CL1 and CX3CR1 in inflammatory foci are accompanied by global activation of both CX3CL1-negative astroglial cells and CX3CL1-negative/CX3CR1-positive microglial cells, which is only partially reversed by 6-Cl-ddG.

Cellular Sources and Plasticity of CX3CL1 and CX3CR1 in the Brain During the Course of Simian Immunodeficiency Virus Disease

Neurons are the predominant source of CX3CL1 in the normal monkey brain as they are in rodent and human brain (11, 12, 17, 19). The transcript and protein of CX3CL1 can clearly be localized in neuronal cell bodies. In accordance with data on rodents (14, 15), microglia in rhesus monkey brain are shown to express CX3CR1. Endothelial cells are another source of CX3CL1 in the rhesus monkey brain in contrast to rodents.

Constitutive neuronal and endothelial CX3CL1 expression is unaltered in early stages of SIV infection. On clinical manifestation of AIDS, there is a widespread neuronal downregulation and a striking focal induction of CX3CL1 in a subset of reactive astrocytes and reactive cells of mononuclear origin in and around areas of SIV burden and inflammation. CX3CL1 mRNA is induced in endothelial cells mainly in areas of virus infiltrates and enhanced in diffusely distributed microglia/macrophages, macrophage nodules, multinucleated giant cells, and monocytic infiltrates in terminal SIV infection with AIDS.

An increase in neuronal CX3CL1 expression, without changes in astrocytes, has been reported in pediatric AIDS brain (22). A global increase in CX3CL1 expression in astrocytes was reported in adult HIV-1 encephalitic brain (23). Our results, combining both immunohistochemistry and in situ hybridization histochemistry and carefully controlling for age, fixation conditions, and stage of disease, demonstrate the expression of CX3CL1 protein and mRNA in neurons of normal uninfected primate brain; downregulation of neuronal CX3CL1 protein and mRNA in late-stage SIV infection and AIDS; and reversal with the central nervous system-permeant antiretroviral 6-Cl-ddG of suppressed CX3CL1 expression during SIV infection. The global reduction of CX3CL1 in neurons, and its focal induction in astrocytes reported here may be a general feature of primate lentiviral encephalitis that is observed more reliably in rhesus brain as a result of greater control over fixation conditions favoring greater sensitivity and specificity of immuno- and in situ hybridization histochemical detection and may in part reflect differences in HIV and SIV disease progression. Our in vivo study of SIV infection contrasts with the demonstration of increased CX3CL1 expression in neurons on in vitro exposure to HIV-1 progeny virions, *gp120* and/or proinflammatory cytokines (21). The differences might be the result of the fact that this work is acutely done in culture compared with the present chronic in situ monkey study rather than reflecting biologic differences between species, their reactions, and the viruses studied.

Influence of Antiretroviral Treatment With 6-Cl-ddG on CX3CL1 and CX3CR1 Expression and Inflammatory Responses

The regulation of CX3CL1 expression in the brain during SIV infection is directly related to virus burden and inflammation. Antiretroviral treatment with 6-Cl-ddG blocks both ongoing viral replication and manifestations of SIV-induced encephalitis, including mononuclear infiltrates, macrophage nodules and multinucleated giant cells, focal upregulation of CX3CL1 in astrocytes and macrophages, and global downregulation of CX3CL1 in neurons. Global activation of astrocytes, however, as evidenced by GFAP expression in CX3CL1-negative astrocytes in both grey and white matter, is only partially reversed by antiretroviral treatment, suggesting a component of early, and irreversible, in addition to ongoing effects of lentiviral infection. The same may be true for microglial activation as evidenced by upregulation of fractalkine receptor CX3CR1 (this study) and complement component C1q (26).

Possible Role of CX3CL1 and CX3CR1 During Brain Simian Immunodeficiency Virus Infection

The widespread downregulation of neuronal CX3CL1 throughout the brain, especially in the cortex and striatum demonstrated here, may decrease brain capacity for neuroprotection during SIV infection in at least 2 ways. First, given the antiapoptotic effect of CX3CL1 on neurons (33), the neuronal downregulation of CX3CL1 after SIV infection could contribute to neuronal death that occurs in neuro-AIDS. Second, reduced brain levels of CX3CL1 could lead to loss of control of microglial toxicity recently demonstrated to be CX3CR1-dependent (34).

The focal induction of CX3CL1 is directly linked to the focal inflammatory processes during SIV infection. We detected focal CX3CL1-positive astrocytes mostly juxtavascular to infiltrates and areas of viral burden. Therefore, it is likely that the focal astrocytes exhibiting induction of CX3CL1 regulate the recruitment of peripheral inflammatory cells into the brain according to the known chemokinetic function of CX3CL1 similar to that previously shown for MCP-1 in HIV-induced encephalitis (35). Fong et al have reported that peripheral endothelial cells synthesize CX3CL1, which enhances chemokinesis and adhesion of CX3CR1-positive cells (36). CX3CL1 produced by brain endothelial cells during SIV infection may similarly contribute to increased infiltration of CX3CR1-bearing cells from the blood stream into the brain.

The induction of CX3CL1 in focal reactive astrocytes is in accordance with the potential of cultured astrocytes to respond to TNF-α and interleukin-1β stimulation with marked CX3CL1 expression (37). CX3CL1 expression in cultured astrocytes is increased synergistically by TNF-α and interferon-γ, resulting in enhanced release of the soluble domain of CX3CL1 into the lysate of the culture (38). Thus, SIV-induced CX3CL1 biosynthesis may be both initiated

and sustained by these proinflammatory cytokines known to be increased in the monkey brain during SIV infection (39). The restriction of increased CX3CL1 biosynthesis to areas of productive inflammation and virus replication may be the result of the fact that these cytokines are particularly expressed in these areas (39). It is also possible that locally produced virus proteins like *tat* or *gp120* (21) as well as metabolites like quinolinic acid from nodule- and giant cell-forming macrophages might also induce CX3CL1 (25, 40).

Garcia et al have reported that CX3CL1 gene transcription on exposure to the cytokines interleukin-1β and TNF-α in aortic endothelial cells is NF-κB-dependent (41). We report here that nuclear localization of NF-κB is a prominent feature of CX3CL1-positive astrocytes and macrophages, suggesting NF-κB as the transcription factor mediating CX3CL1 induction in these cells, potentially triggered by the same cytokines.

CONCLUSION

Our results suggest that CX3CL1 could be critically involved in local inflammatory processes in the SIV-diseased brain as summarized in Figure 9. Downregulation of neuronal CX3CL1 expression, correlated with SIV burden, may result in impaired control of microglial neurotoxicity. CX3CL1 focally induced in astrocytes may aid recruitment of CX3CR1-positive blood-derived cells during SIV infection of the brain.

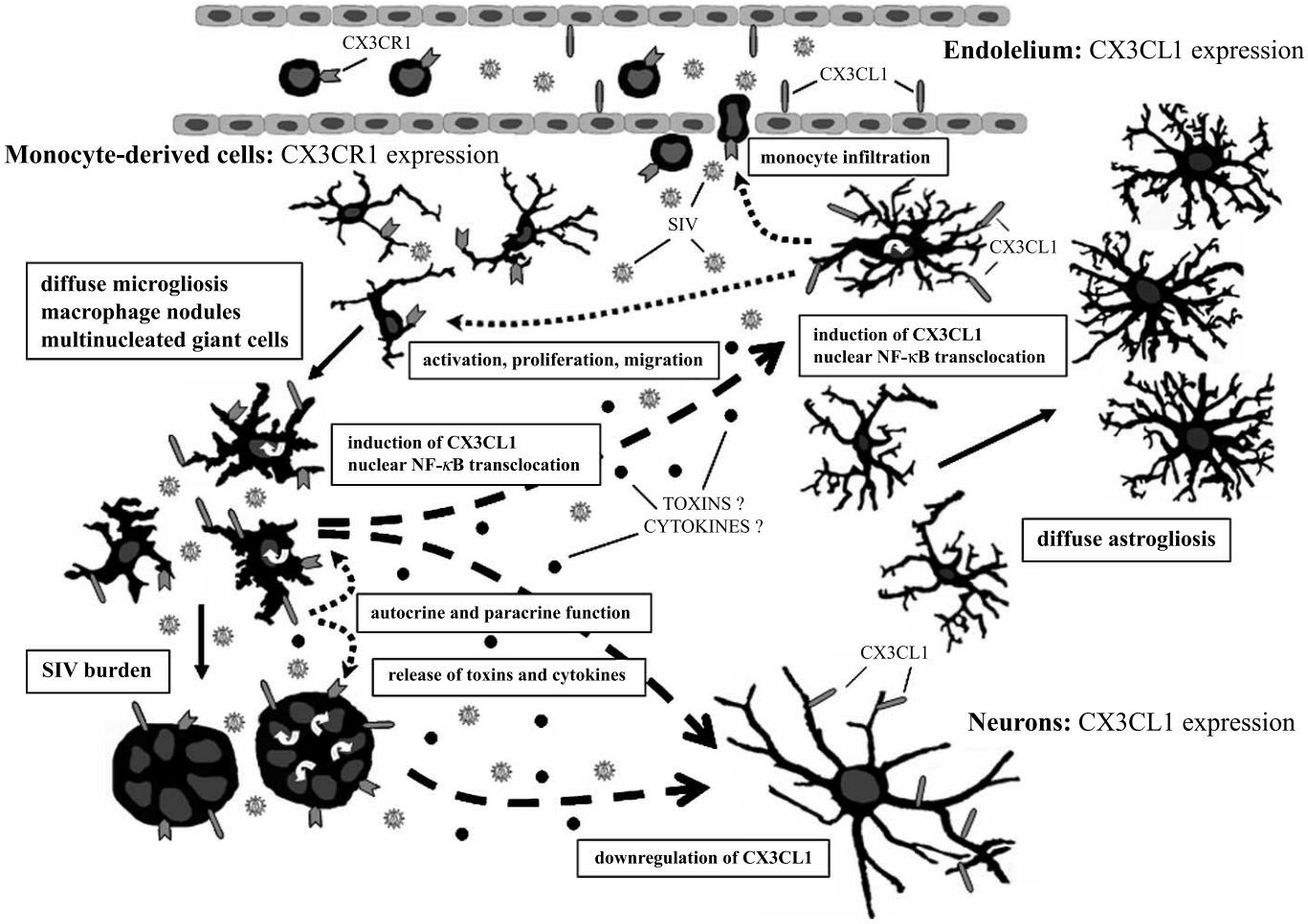

FIGURE 9. Schematic diagram illustrating a hypothetical model of the cellular interactions through the CX3CL1-CX3CR1 pathway in lentiviral encephalopathy. CX3CL1 is expressed in neurons and endothelial cells. CX3CR1 is produced by microglia. CX3CL1 is downregulated in neurons, and focally induced in astrocytes and macrophages in areas with SIV burden. In some endothelial cells, CX3CL1 is upregulated. In parallel, CX3CR1 is increased in cells of monocyte/macrophage origin that become activated and infiltrating into brain, mainly in those areas where CX3CL1 is newly produced. SIV-driven, focally released substances may cause expression of CX3CL1 in astrocytes and macrophages through NF-κB. It is postulated that focally induced CX3CL1 promotes infiltration of CX3CR1-positive monocytes through the blood–brain barrier from the systemic circulation and activates nearby CX3CR1-positive microglia. In addition, CX3CL1 in CX3CR1-positive macrophages may have autocrine and paracrine effects to maintain their activation state. This dynamic and complex interplay between CX3CL1 and CX3CR1 may be directly and/or indirectly involved in the global activation of the inflammatory response and spreading of SIV infection within the brain. Downregulation of CX3CL1 expression in neurons may result in reduced control of microglial/macrophage toxicity in neuro-AIDS.

Central nervous system-permeant antiretroviral treatment reverses viral burden, focal induction of CX3CL1 in inflammatory cells and astrocytes, as well as neuronal loss of CX3CL1 expression, whereas global microglial and astroglial responses are only partially susceptible to 6-Cl-ddG. This suggests 2 distinct phases of lentiviral neuropathogenesis, one is an inflammatory metabolic pathway dependent on virus burden and reversed by antiretroviral treatment even in late SIV disease, and a second possibly degenerative pathway involving global microglial and astroglial activation, only partially reversed by central nervous system-directed antiretroviral therapy when administered late in SIV disease. Disruption of CX3CL1-CX3CR1-mediated cellular communication may be a therapeutic target to block infected macrophage trafficking to the brain and to prevent brain injury secondary to inflammatory cell infiltration, especially early in the course of disease.

ACKNOWLEDGMENTS

For excellent technical work, the authors are indebted to R. Vertesi from L. E. Eiden's laboratory and E. Rodenberg-Frank, M. Zibuschka, H. Hlawaty, and H. Schneider from E. Weihe's laboratory.

Parts of this study were presented at the Annual Meeting of the Society for Neuroscience, 2002(42).

REFERENCES

1. Murray EA, Rausch DM, Lendvay J, et al. Cognitive and motor impairments associated with SIV infection in rhesus monkeys. Science 1992;255:1246–49
2. Budka H. Multinucleated giant cells in the brain: A hallmark of the acquired immunodeficiency syndrome (AIDS). Acta Neuropathol (Berl) 1986;69:253–58
3. Weihe E, Nohr D, Sharer L, et al. Cortical astrocytosis in juvenile rhesus monkeys infected with simian immunodeficiency virus. Neuroreport 1993;4:263–66
4. Lane JH, Sasseville VG, Smith MO, et al. Neuroinvasion by simian immunodeficiency virus coincides with increased numbers of perivascular macrophages/microglia and intrathecal immune activation. J Neurovirol 1996;2:423–32
5. Luabeya MK, Dallasta LM, Achim CL, et al. Blood–brain barrier disruption in simian immunodeficiency virus encephalitis. Neuropathol Appl Neurobiol 2000;26:454–62
6. Luthert PJ, Montgomery MM, Dean AF, et al. Hippocampal neuronal atrophy occurs in rhesus macaques following infection with simian immunodeficiency virus. Neuropathol Appl Neurobiol 1995;21:529–34
7. Li Q, Eiden LE, Cavert W, et al. Increased expression of nitric oxide synthase and dendritic injury in simian immunodeficiency virus encephalitis. J Hum Virol 1999;2:139–45
8. Bissel SJ, Wang G, Ghosh M, et al. Macrophages relate presynaptic and postsynaptic damage in simian immunodeficiency virus encephalitis. Am J Pathol 2002;160:927–41
9. Glass JD, Fedor H, Wesselingh SL, et al. Immunocytochemical quantitation of human immunodeficiency virus in the brain: Correlations with dementia. Ann Neurol 1995;38:755–62
10. Springer TA. Traffic signals for lymphocyte recirculation and leukocyte emigration: The multistep paradigm. Cell 1994;76:301–14
11. Bazan JF, Bacon KB, Hardiman G, et al. A new class of membrane-bound chemokine with a CX3C motif. Nature 1997;385:640–44
12. Pan Y, Lloyd C, Zhou H, et al. Neurotactin, a membrane-anchored chemokine upregulated in brain inflammation. Nature 1997;387:611–17
13. Zlotnik A, Yoshie O. Chemokines: A new classification system and their role in immunity. Immunity 2000;12:121–27
14. Imai T, Hieshima K, Haskell C, et al. Identification and molecular characterization of fractalkine receptor CX3CR1, which mediates both leukocyte migration and adhesion. Cell 1997;91:521–30
15. Combadiere C, Salzwedel K, Smith ED, et al. Identification of CX3CR1: A chemotactic receptor for the human CX3C chemokine fractalkine and a fusion coreceptor for HIV-1. J Biol Chem 1998;273:23799–804
16. Harrison JK, Barber CM, Lynch KR. cDNA cloning of a G-protein-coupled receptor expressed in rat spinal cord and brain related to chemokine receptors. Neurosci Lett 1994;169:85–89
17. Harrison JK, Jiang Y, Chen S, et al. Role for neuronally derived fractalkine in mediating interactions between neurons and CX3CR1-expressing microglia. Proc Natl Acad Sci U S A 1998;95:10896–901
18. Nishiyori A, Minami M, Ohtani Y, et al. Localization of fractalkine and CX3CR1 mRNAs in rat brain: Does fractalkine play a role in signaling from neuron to microglia? FEBS Lett 1998;429:167–72
19. Schwaeble WJ, Stover CM, Schall TJ, et al. Neuronal expression of fractalkine in the presence and absence of inflammation. FEBS Lett 1998;439:203–207
20. Sporer B, Kastenbauer S, Koedel U, et al. Increased intrathecal release of soluble fractalkine in HIV-infected patients. AIDS Res Hum Retroviruses 2003;19:111–16
21. Erichsen D, Lopez AL, Peng H, et al. Neuronal injury regulates fractalkine: Relevance for HIV-1 associated dementia. J Neuroimmunol 2003;138:144–55
22. Tong N, Perry SW, Zhang Q, et al. Neuronal fractalkine expression in HIV-1 encephalitis: roles for macrophage recruitment and neuroprotection in the central nervous system. J Immunol 2000;164: 1333–39
23. Pereira CF, Middel J, Jansen G, et al. Enhanced expression of fractalkine in HIV-1 associated dementia. J Neuroimmunol 2001;115:168–75
24. Fujii Y, Mukai R, Akari H, et al. Antiviral effects of 6-chloro-2′,3′-dideoxyguanosine in rhesus monkeys acutely infected with simian immunodeficiency virus. Antivir Chem Chemother 1998;9:85–92
25. Depboylu C, Reinhart TA, Takikawa O, et al. Brain virus burden and indoleamine-2,3-dioxygenase expression during lentiviral infection of rhesus monkey are concomitantly lowered by 6-chloro-2′,3′-dideoxygenosine. Eur J Neurosci 2004;19:2997–3005
26. Depboylu C, Schäfer MK-H, Schwaeble WJ, et al. Increase of C1q biosynthesis in brain microglia and macrophages during lentivirus infection in the rhesus macaque is sensitive to antiretroviral treatment with 6-chloro-2′,3′-dideoxyguanosine. Neurobiol Dis 2005;20:12–26
27. da Cunha A, Rausch DM, Eiden LE. An early increase in somatostatin mRNA expression in the frontal cortex of rhesus monkeys infected with simian immunodeficiency virus. Proc Natl Acad Sci U S A 1995; 92:1371–75
28. Imai Y, Ibata I, Ito D, et al. A novel gene iba1 in the major histocompatibility complex class III region encoding an EF hand protein expressed in a monocytic lineage. Biochem Biophys Res Commun 1996; 224:855–62
29. Basu S, Schaefer TM, Ghosh M, et al. Molecular cloning and sequencing of 25 different rhesus macaque chemokine cDNAs reveals evolutionary conservation among C, CC, CXC, AND CX3C families of chemokines. Cytokine 2002;18:140–48
30. Schäfer MK-H, Day R. In situ hybridization techniques to study processing enzyme expression at the cellular level. Methods Neurosci 1994;23:16–44
31. Kent KA, Rud E, Corcoran T, et al. Identification of two neutralizing and eight non-neutralizing epitopes on simian immunodeficiency virus envelope using monoclonal antibodies. AIDS Res Hum Retroviruses 1992;8:1147–51
32. Reinhart TA, Rogan MJ, Huddleston D, et al. Simian immunodeficiency virus burden in tissues and cellular compartments during clinical latency and AIDS. J Infect Dis 1997;176:1198–208
33. Deiva K, Geeraerts T, Salim H, et al. Fractalkine reduces N-methyl-D-aspartate-induced calcium flux and apoptosis in human neurons through extracellular signal-regulated kinase activation. Eur J Neurosci 2004;20:3222–32
34. Cardona AE, Pioro EP, Sasse ME, et al. Control of microglial neurotoxicity by the fractalkine receptor. Nat Neurosci 2006;9:917–24
35. Conant K, Garzino-Demo A, Nath A, et al. Induction of monocyte chemoattractant protein-1 in HIV-1 Tat-stimulated astrocytes elevation in AIDS dementia. Proc Natl Acad Sci U S A 1998;95:3117–21

36. Fong AM, Robinson LA, Steeber DA, et al. Fractalkine and CX3CR1 mediate a novel mechanism of leukocyte capture, firm adhesion, and activation under physiologic flow. J Exp Med 1998;188: 1413–19
37. Maciejewski-Lenoir D, Chen S, Feng L, et al. Characterization of fractalkine in rat brain cells: Migratory and activation signals for CX3CR-1-expressing microglia. J Immunol 1999;163:1628–35
38. Yoshida H, Imaizumi T, Fujimoto K, et al. Synergistic stimulation, by tumor necrosis factor-alpha and interferon-gamma, of fractalkine expression in human astrocytes. Neurosci Lett 2001;303:132–36
39. Orandle MS, MacLean AG, Sasseville VG, et al. Enhanced expression of proinflammatory cytokines in the central nervous system is associated with neuroinvasion by simian immunodeficiency virus and the development of encephalitis. J Virol 2002;76:5797–802
40. Guillemin GJ, Croitoru-Lamoury J, Dormont D, et al. Quinolinic acid upregulates chemokine production and chemokine receptor expression in astrocytes. Glia 2003;41:371–81
41. Garcia GE, Xia Y, Chen S, et al. NF-kappaB-dependent fractalkine induction in rat aortic endothelial cells stimulated by IL-1beta, TNF-alpha, and LPS. J Leukoc Biol 2000;67:577–84
42. Weihe E, Depboylu C, Rausch DM, et al. Fractalkine biosynthesis in rhesus macaque brain: cell specific regulation in SIV infection and effect of antiretroviral treatment [Abstract]. Soc Neurosci Abstr 2002; 28:395–11